[25] Brown, D., Mokry, M., and Ohman, L. H., "Further Calibration of the 15″ × 60″ Two-Dimensional Test Facility with 6% Open Floor and Ceiling at the Test Section," Project Rept. 5 × 5/0050, Sept. 1971, NRC, Ottawa, Canada.

[26] Sells, C. C. L., "Plane Subcritical Flow past a Lifting Airfoil," *Proceedings of the Royal Society*, Series A. 308, 1968, pp. 371–401.

[27] Kacprzynski, J. J., "Fortran IV Program for the Catherall-Foster-Sells Method for Calculation of the Plane Inviscid Incompressible Flow past a Lifting Aerofoil," LTR-HA-2, April 1970, NRC, Ottawa, Canada.

[28] Kacprzynski, J. J., "Fortran IV Program for the Sells Method for Subcritical Two-Dimensional Inviscid Flow Calculations past a Lifting Aerofoil," LTR-HA-3, April 1970, NRC, Ottawa, Canada.

[29] Mokry, M., "Calculation of Flow Past Multi-Component Airfoils in Perforated Wind Tunnel," *Proceedings of the 4th Canadian Congress of Applied Mechanics*, Montreal, May 1973.

JANUARY 1975 AIAA JOURNAL VOL. 13, NO. 1

Comparison of Pressure and LDV Velocity Measurements with Predictions in Transonic Flow

RONALD D. FLACK,* AND H. DOYLE THOMPSON†
Purdue University, West Lafayette, Ind.

This paper presents a comparison of the sonic line location in a series of two-dimensional nozzles as determined by static pressure measurements, Laser Doppler Velocimeter (LDV) velocity measurements, and an analytical solution based on a series expansion. Wall static pressure data have been obtained for 13 different two-dimensional nozzles, including 10 unsymmetrical nozzles. An LDV has been designed, built, and used to make extensive flow velocity measurements in two of the nozzles. The system uses a 4 w argon laser in a forward scatter, dual beam configuration. The analytical solution is based on a series expansion in terms of the wall geometry in the transonic region and is developed for annular as well as two-dimensional inviscid internal flows. The analytical sonic line location is slightly upstream of the experimental sonic line based on static pressure measurements in all thirteen of the nozzles examined. The difference for the nozzles tested is between 1 and 4% (based on Mach number) and is largely attributable to the neglecting of boundary-layer effects in the analytical model. The sonic lines based on LDV measurements fall between the analytical and static pressure sonic lines. The agreement is excellent. The experimental and analytical data confirm that transonic flows may be sensitive to small changes in the flow boundaries, and indicate that the sonic line location in annular nozzles (i.e., plug and forced deflection nozzles), and in unsymmetric two-dimensional nozzles may be very different from the essentially one-dimensional uniform flow that is commonly assumed.

Introduction

TRANSONIC flow has been found to be very dependent on the flow boundaries in that small changes in a flow boundary may dramatically alter the entire flowfield. This nonlinear behavior leads to many interesting problems, not only in the analysis and design of transonic flow passages, but also in the accurate measurement of pressures and velocities in transonic flowfields. There are numerous applications in the fields of jet propulsion, turbomachinery, fluidics, and others. One problem that is partially responsible for the present research is the determination of an accurate supersonic start line in an annular nozzle from which a method of characteristics solution can be initiated. Another application arises in the design and flow analysis in high performance compressors in which the cascades perform as a series of unsymmetric nozzles. Very often a portion of the flowfield is in the transonic range. Although the flow is three-dimensional, the solution for a two-dimensional unsymmetrical transonic flowfield is a useful and important approximation to the actual flow.

Analytically, the problem of internal transonic flow has been examined by several methods. Sauer,[1] Hall,[2] Kleigel and Levine,[3] Levine and Coats,[4] and Moore and Hall[5] have used small perturbation approaches for inviscid nozzles. More recently, Thompson and Flack[6-7] have applied the approach to unsymmetric two-dimensional and annular nozzles. Results from Refs. 6 and 7 are included herein.

Serra[8] and Wehofer and Moger[9] have used asymptotic steady-state solutions to the time-dependent equations to determine the transonic flowfield in two-dimensional and annular axisymmetric nozzles. Brunell[10] used the time-dependent solution for two-dimensional nozzles, and Prozan and Kooker[11] used an error minimization relaxation scheme for axisymmetric nozzles to obtain the steady-state solution. Holt[12] and Liddle and Archer[13] have used the Method of Integral Equations in solving two-dimensional and axisymmetric flow problems. Hopkins and Hill[14,15] implemented an inverse method originally formulated by Friedrichs.[16] The work has been supplemented by the work of Morden and Farquhar[17] and is applicable to conventional and annular nozzles.

Experimentally, only a small amount of data involving internal transonic flow has been published. A major portion of this data is wall-static pressure measurements. Jacobs[18] experiment-

Presented as Paper 74-15 at the AIAA Aerospace Sciences Meeting, Washington, D.C., January 30–February 1, 1974; submitted February 14, 1974; revision received June 28, 1974. This work was sponsored by the U.S. Army Missile Command, Redstone Arsenal, Ala., under Contract DAAH01-72-C-0089.

Index categories: Subsonic and Transonic Flow; Nozzle and Channel Flow.

* Graduate Research Assistant. Student Member AIAA.

† Professor. Member AIAA.

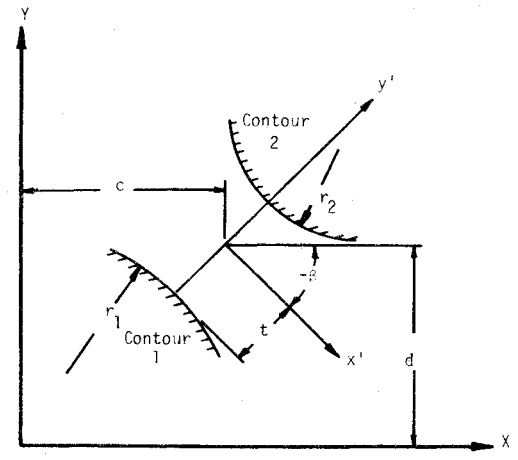

Fig. 1 Geometry for typical two-dimensional or annular nozzle.

ally examined six unsymmetric, two-dimensional converging-diverging nozzles. At the Jet Propulsion Lab., measurements have been made in several axisymmetric nozzles by Back and his associates.[19-22] Wall-static pressure data have recently been obtained for 13 two-dimensional nozzles including 10 unsymmetric nozzles. The data, complimented with Laser Doppler Velocimeter data for two of the nozzles, are presented here.

Analytical Method

The analytical results presented here are based on a mathematical technique which uses an asymptotic expansion for the flow variables in terms of an expansion parameter ε. The expansion parameter is determined by the wall geometry in the immediate neighborhood of the throat (minimum flow area). The method is described in detail in Ref. 6 which also serves as a computer manual for the computer program. The analysis and computer program were developed to treat both two-dimensional and annular, axisymmetric transonic flows. The flow boundaries may be symmetric or unsymmetric. The method is conceptually similar to, but more general than, the works of Hall,[2] Kleigel and Levine,[3] and Moore and Hall.[5]

Space limitations preclude the inclusion of even the final equations for the computation. However, to understand the conclusions it is didactic to consider the method from a general point of view. In the course of the derivation, assumptions were made which are normal for this type of flow. These are that the flow is inviscid, irrotational, and nonreacting; that heat transfer within the gas and to the surroundings can be neglected; that the gas is calorically and thermally perfect; and that the flow channel is choked. Figure 1 depicts a typical geometry. The X and Y coordinates are along and radial to the axis of symmetry, respectively, for an axisymmetric flow. The expansion is performed in the transformed x', y' coordinate system where y' is along the line which defines the minimum flow area and x' is normal to y' with the origin equidistant from the boundaries 1 and 2. The positive x' direction is along the main flow direction. In a two-dimensional flow the x', y' coordinates are the primary coordinates and the minimum area line coincides with the minimum distance between curves 1 and 2. For annular axisymmetric flow in which $\beta \neq 0$ the minimum flow area line is different from the minimum distance line.

All lengths are nondimensionalized by the half throat height t (i.e., $x = x'/t$, $y = y'/t$, etc.). The perturbation velocities u and v (in the x and y directions, respectively) have been nondimensionalized by the sonic velocity a^* and are expanded in powers of an expansion parameter ε in the form

$$u = u_1\varepsilon + u_2\varepsilon^2 + u_3\varepsilon^3 + \ldots \tag{1}$$

$$v = v_1\varepsilon^{3/2} + v_2\varepsilon^{5/2} + v_3\varepsilon^{7/2} + \ldots \tag{2}$$

where

$$\varepsilon \cong \frac{1}{2}\left[\frac{1}{R_1+\eta} + \frac{1}{R_2+\eta}\right] \tag{3}$$

and where η may be 0 or 1, resulting in expansion parameters like $1/R$ and $1/(R+1)$, respectively.

R is the nondimensional radius of curvature of a contour at the minimum area (i.e., $R = r/t$). The subscripts on R refer to contours 1 and 2, respectively (see Fig. 1). The subscripts on u and v (1, 2, and 3) refer to the component order.

The basic gas dynamic equations used are the irrotationality relationship, the differential forms of the continuity, isentropic, and energy equations, and a transform of axes. The irrotationality condition becomes

$$\partial u/\partial y = \partial v/\partial x \tag{4}$$

The continuity, isentropic, and energy equations are combined and become

$$-A_1\,\partial u/\partial x - A_2\,\partial u/\partial y + A_3\,\partial v/\partial y + \sigma T = 0 \tag{5}$$

where σ equals 0 for two-dimensional flow and 1 for annular axisymmetric flow. A_1, A_2, A_3, and T functions of u, v, the specific heat ratio, γ, and geometry, and are defined in Ref. 6.

Upon substitution of Eqs. (1) and (2) into Eqs. (4) and (5), and grouping like powers of ε one obtains the following:

$$\varepsilon(\partial u_1/\partial y - \partial v_1/\partial z) + \varepsilon^2(\partial u_2/\partial y - \partial v_2/\partial z) + \varepsilon^3(\partial u_3/\partial y - \partial v_3/\partial z) + \ldots = 0 \tag{6}$$

$$J_1\varepsilon^{3/2} + J_2\varepsilon^{5/2} + J_3\varepsilon^{7/2} + \ldots = 0 \tag{7}$$

where

$$J_1 = -2u_1(\partial u_1/\partial z) + \Psi(\partial v_1/\partial y) + \Psi K \tag{8}$$

and where $z = x\varepsilon^{-1/2}$. J_2 and J_3 are partial differential equations with dependent variables u_2, v_2 and u_3, v_3, respectively, and are derived in Ref. 6. Ψ is a function of the specific heat ratio and K is a function of the geometric parameters. After some manipulation the boundary conditions corresponding to Eqs. (6) and (7) can be written in the form

$$\varepsilon^{3/2}[v_1(z,1) - (m_1+m_2z)] + \varepsilon^{5/2}[v_2(z,1) - (m_1+m_2z)(u_1(z,1)+\eta)] + \varepsilon^{7/2}\{v_3(z,1) + (z/2)\times(2m_1+m_2z)(\partial v_1/\partial y)|_{z,1} - (m_1+m_2z)[u_2(z,1) + \eta u_1(z,1) + \eta]\} + \ldots = 0 \tag{9}$$

$$\varepsilon^{3/2}[v_1(z,-1) + (n_1+n_2z)] + \varepsilon^{5/2}[v_2(z,-1) + (n_1+n_2z)(u_1(z,-1)+\eta)] + \varepsilon^{7/2}\{v_3(z,-1) - (z/2)(2n_1+n_2z)(\partial v_1/\partial y)|_{z,-1} + (n_1+n_2z)[u_2(z,-1) + \eta u_1(z,-1) + \eta]\} + \ldots = 0 \tag{10}$$

where m_1 and m_2 are functions of R_2, and n_1 and n_2 are functions of R_1. To obtain a solution, the coefficients of the full power ε terms in Eqs. (6) and (7) are set equal to zero and these equations are solved along with the corresponding boundary conditions. For example for the first-order solution the equations

$$\partial u_1/\partial y = \partial v_1/\partial z \tag{11}$$

$$J_1 = -2u_1(\partial u_1/\partial z) + \Psi(\partial v_1/\partial y) + \Psi K = 0 \tag{12}$$

with the boundary conditions

$$v_1(z,1) - (m_1+m_2z) = 0 \tag{13}$$

and

$$v_1(z,-1) + (n_1+n_2z) = 0 \tag{14}$$

are solved by assuming a series solution to obtain $u_1(x,y)$ and $v_1(x,y)$.

For the second-order solution, the equations

$$\partial u_2/\partial y = \partial v_2/\partial z \tag{15}$$

$$J_2(u_1, u_2, v_1, v_2, z, y, \varepsilon) = 0 \tag{16}$$

with the boundary conditions

$$v_2(z,1) - [m_1+m_2z][u_1(z,1)+\eta] = 0 \tag{17}$$

and

$$v_2(z,-1) + [n_1+n_2z][u_1(z,-1)+\eta] = 0 \tag{18}$$

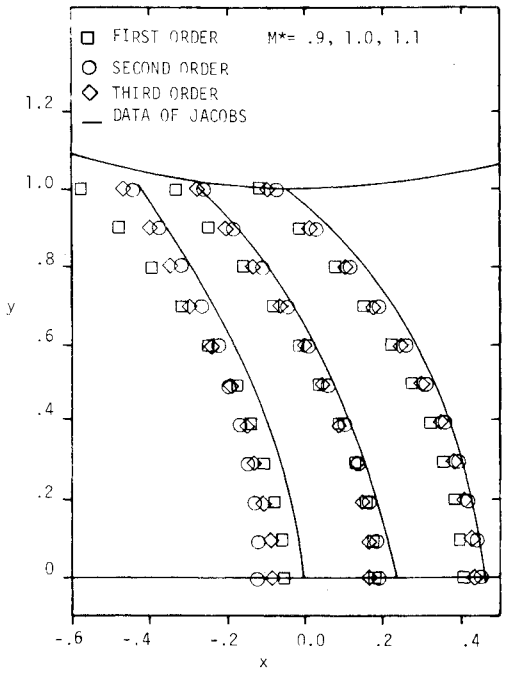

Fig. 2 Comparison of first, second, and third-order analytical solutions and the data of Jacobs for nozzle T2-2F.

are solved using the first-order solution to obtain $u_2(x, y)$ and $v_2(x, y)$. The third-order solution is obtained in an analogous manner.

An important feature of the approach is that several truncated series expansions have been made around $x = 0$, $y = 0$, and $M = 1.0$. Consequently, the series solutions are valid representations of the flow variables only in a limited region sufficiently close to $x = 0$, $y = 0$, and $M = 1$. The hope is that the region of valid results is sufficiently large to permit a "supersonic start line" to be established. The region of valid results is determined by the boundary geometry (i.e., values of R_1 and R_2), the number of terms retained in the truncated series, and the form of the series. In Refs. 6 and 7 a limited study is reported in which three orders of accuracy are computed and the effects of η are investigated for a variety of two-dimensional and annular axisymmetric geometries. Briefly, the results of that study are that the third-order solution usually appears to be the most accurate.‡ The value of η (i.e., 0 or 1) has little effect for values of R_1 and R_2 greater than about 2.5, but using $\eta = 1$ appears to extend the region of valid results for smaller values of R_1 and R_2. For values of R less than about 0.5 (based on symmetry) the region of valid results is not sufficient to establish a good supersonic start line. The limitations are more severe for nonsymmetric geometries.

To illustrate the method, results for a two-dimensional and an annular nozzle are presented (η equals unity for all cases). Figure 2 shows a nozzle with a flat lower surface, an upper surface with a radius of 2 units, and a throat height of one unit. Isomachs of 0.90, 1.00, and 1.10 are presented for the first, second, and third-order solutions. One feature of the method is demonstrated. Equation (1) tends to be an alternating series. In Fig. 2 this behavior is evident as the third-order solution falls between the first and second-order solutions. Comparison of the three orders has been made with the data of Jacobs.[18]

The annular flow case is presented in Fig. 3. The geometry has two walls with equal radii of 0.625 units, a half-throat height of unity and distance to the centerline of 10 units. Isomachs of 0.90, 1.00, and 1.10 are presented for second and third-order analytical solutions for $\eta = 1$. The analytical solution is well behaved even though the dimensionless wall radii of curvature are considerably less than unity. The analytical solutions for several other two-dimensional geometries will later be compared to the experimental results in Figs. 9, 10, and 11.

Over all, the theoretical method produces meaningful results for a large range of practical annular and two-dimensional flow geometries. The method is straightforward and requires very little computer time as compared to the more elaborate time-dependent or inverse methods. The representative computer time for a normal calculation on the Purdue Univ. CDC 6500 computer is 10 sec.

‡ There are some geometries for which the basic series is apparently diverging for larger values of y such that the third-order solution is obviously incorrect but the first and second-order solutions appear to be plausible.

Experimental Apparatus

The experimental test facility consists of a blowdown air system, a plenum chamber, and a two–dimensional nozzle. The first nozzle used was symmetric with circular arc contours for the boundaries and flat Plexiglas sidewalls. The boundaries were machined from stainless steel and have radii of curvature of 3.000 ± 0.003 in. The throat height, $2t$, is 1.005 ± 0.003 in. and the width of the flow channel is 1.000 ± 0.003 in. The blocks were instrumented with 0.018 in. diam staggered pressure taps. Sixteen taps were drilled approximately 0.100 in. apart axially, spanning the transonic region on the upper wall. On the lower wall a single tap was drilled at 0.062 in. upstream of the one-dimensional throat. The positions of the centers of the taps were measured to within ± 0.003 in. These taps lead to a 48 port Scanivalve-Statham transducer combination from which the output is recorded on digital tape.

One of the Plexiglas sidewalls was also instrumented with 0.018 in. diam pressure taps in three staggered rows spanning the flow passage in both the x and y directions. The x and y positions of the centers of these taps were measured to within ± 0.010 in. The sidewall taps also lead to the Scanivalve.

One advantage of using a modular construction is that a variety of different configurations can be achieved by replacing one nozzle block and/or adjusting the throat height. Thirteen nozzles have been experimentally examined in this work using five different nozzle blocks in various combinations and spacings. Table 1 lists the geometry of the 13 nozzles which are identified by a numbering system which indicates the geometry. The

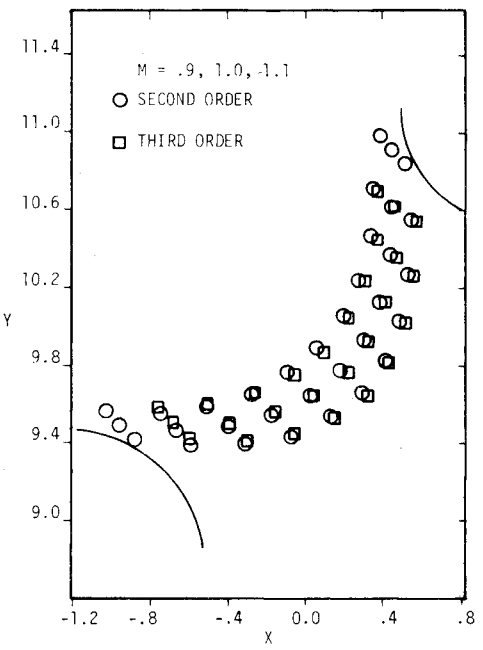

Fig. 3 Analytical solution for annular axisymmetric flow in nozzle A.625-.625.

Table 1 Two-dimensional nozzle configurations

Designation	Upper wall radius r_2 (in.)	Lower wall radius r_1 (in.)	Half throat height t (in.)
T6-6	3.000	3.000	0.503
T4-4	3.000	3.000	0.725
T3-3	3.000	3.000	1.000
T6-6F	3.000	inf.[a]	0.503[c]
T3-3F	3.000	inf.[a]	1.000[c]
T2-2F	3.000	inf.[a]	1.500[c]
T1.5-1.5F	3.000	inf.[a]	2.000[c]
T12-24I	3.000	6.100[b]	0.250
T4-8I	3.000	6.100[b]	0.750
T3-6I	3.000	6.100[b]	1.000
T12-24	3.000	6.000	0.250
T4-8	3.000	6.000	0.750
T3-6	3.000	6.000	1.000

[a] Surface is flat.
[b] Curvature is concave.
[c] Half throat height is based on a symmetric contour. Thus, for example, for nozzle T6-6F the flat plate replaces the centerplane in nozzle T6-6 and is 0.503 in. from the upper contour at the throat.

numbering scheme is of the form TR_2-R_1 where R_2 and R_1 are numerical values of the nondimensional upper and lower wall radii, respectively (nondimensionalized by the half throat height t). The letter T indicates the nozzle is two-dimensional, while the letter A denotes an axisymmetric annular nozzle. The letter I immediately following the numerical value of R_1 is used to denote an inverse (concave) curvature, while the letter F is used to denote a flat surface. For example, the first nozzle listed in the table is symmetric, has nondimensionalized radii of curvature $R_1 = R_2 = 5.970$, and is designated T6-6. When the lower contour of that nozzle is replaced by a flat wall at the centerplane of the nozzle, the configuration is designated T6-6F. Thus, nozzles T6-6F, T3-3F, T2-2F, and T1.5-1.5F are actually half nozzles. For each the lower nozzle contour is flat and located at the centerplane of the corresponding symmetrical nozzle.

To complement the static pressure measurements, flow velocity measurements were made with a dual beam forward scatter Laser Doppler Velocimeter (LDV). Operation of the LDV is based on the frequency shift produced when coherent radiation from a laser source is scattered from small, micron size particles moving in the fluid stream. Figure 4 is a simplified schematic of the LDV system used in this investigation. The measurements were made using the 5145 Å line of a 4 w argon laser. Only the axial velocity component was measured. However, the capability to measure a second velocity component using the 4880Å line is being added.

The total included angle between the input beams is 4.2° and the "probe volume" is an ellipsoid approximately 0.2 mm in diam and 1.4 mm long. The optical system and the laser are mounted on a large lathe bed which can be transversed in all three directions.

Signals from the photomultiplier tube are processed by electronics designed by Zammit, Pedigo, and Stevenson.[23] The electronics use advanced solid state components and design to measure the frequency of the Doppler signal by counting "zero crossings." The system is capable of determining frequencies up to 90 MHz. Comparison and descrimination circuitry eliminates "bad" signals. A more detailed description of the electronics is contained in Ref. 23. Output from the electronics is recorded on magnetic tape.

To scatter light and produce the Doppler signal, a seeding system is used similar to that described by Yanta.[24] The seeding material is Dioctyl Phthalate (DOP). A Laskin nozzle with impactor plates is used to generate particles estimated to be 0.5–2 μ in diam. The size distribution will produce a velocity distribution in the measurements since the particle velocity lag in an accelerating flow is a function of the particle size.

Experimental Procedure and Accuracy

Three types of experimental data were taken: 1) wall static pressures along the nozzle contours, 2) wall static pressures on one sidewall, and 3) LDV velocity measurements in the main flow.

The wall static pressure measurements were made for the thirteen nozzle configurations listed in Table 1. All static pressures were measured with a 48-port Scanivalve-Statham transducer combination and were recorded on digital tape. The transducer was calibrated before each run. Forty data samples were recorded and averaged for each pressure reading.

Each run was made at stagnation pressures of approx 90, 115, and 140 psia and the results compared. The results varied less than 1% between runs. The results reported are the average values. The stagnation temp ranged between 10°F and 40°F depending on the day and the run duration. Reproducibility was verified by rerunning several of the nozzles on different days. Again the results varied less than 1%.

Mach numbers corresponding to the static pressure measurements are calculated assuming an isentropic freestream flow and an ideal gas. Thus

$$M = \{2/(k-1)[(p_o/p)^{k-1/k}-1]\}^{1/2} \tag{19}$$

where p is the measured static pressure and p_o is the measured stagnation pressure. The over-all uncertainty in the static and stagnation pressure measurements is less than ± 0.5 psia which corresponds to a maximum uncertainty of less than $\pm 1.25\%$ in the Mach number.

LDV data have been included for two of the nozzles, namely T6-6F and T4-8. Data were taken at 25 and 50 stations, respectively, traversing the transonic region in both the x and y directions. Approximately 1000 LDV data samples

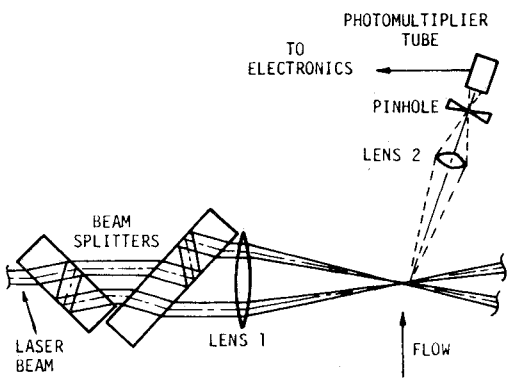

Fig. 4 Schematic of dual scatter LDV.

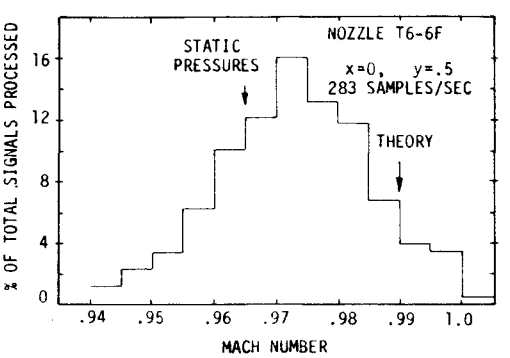

Fig. 5 Histogram of typical LDV data at one flow point.

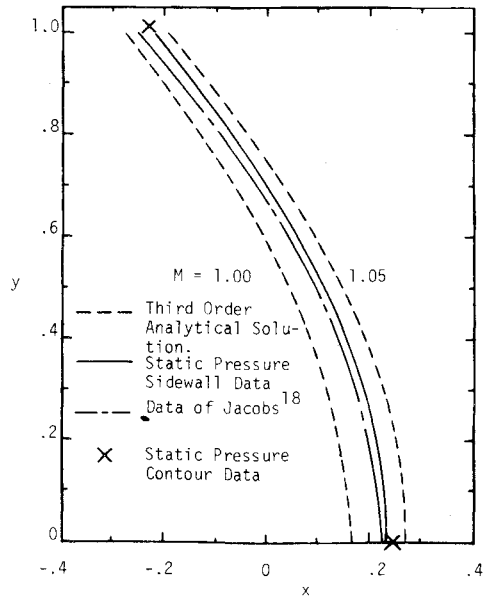

Fig. 6 Comparison of experimental and analytical sonic line location in nozzle T2-2F.

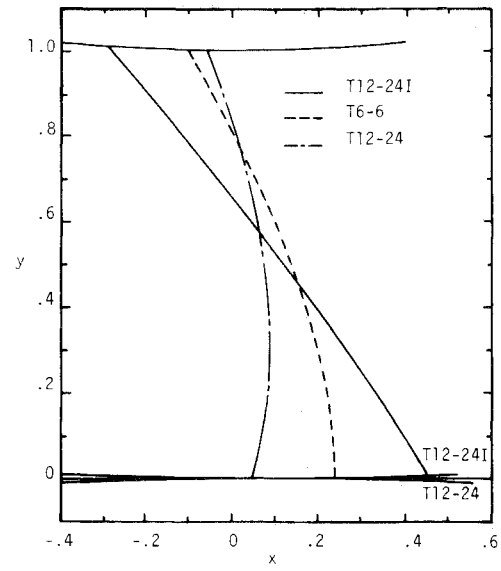

Fig. 8 Comparison of static pressure sonic lines in nozzles T12-24I, T6-6, and T12-24.

were recorded per station. Figure 5 is a typical histogram for approximately 1000 data samples showing the percentage of the total samples with a measured Mach number within an increment of 0.005. The histogram in Fig. 5 is for nozzle T6-6F and represents the data at $x = 0$ and $y = 0.5$. The sample rate of 283 samples/sec is typical. Slower sample rates result from misalignment of the receiving optics and from "tighter" adjustments to the signal processing electronics. Appreciably faster sample rates are precluded at present because of limitations of the data recording system being used. The elctronics package which performs the descrimination and signal processing is capable of a much faster data rate of the order of 10,000 samples/sec.

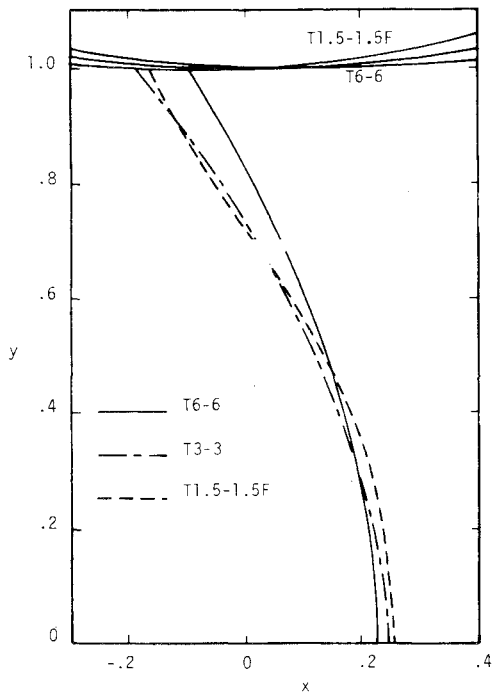

Fig. 7 Comparison of static pressure sonic lines in nozzles T6-6, T3-3, and T1.5-1.5F.

For the LDV system the flow velocity is computed from the measured Doppler shift in the laser light according to the equation

$$V = [f_D \lambda / 2 \sin(\theta/2)] \tag{20}$$

where f_D is the frequency of the signal generated by the photomultiplier tube, λ is the wavelength of the laser light, and θ is the total angle between the incident light beams.

A complete analysis of the accuracy of the LDV system is premature at this time. The shape and spread in the histogram (Fig. 5) is undoubtedly due to several factors including a low level of turbulent fluctuations, a finite discriminator setting on the electronics comparitor circuit (estimated at about 2%), optical aberrations, and variation in particle lag due to a distribution of particle sizes.§ Futhermore, the entire histogram can be shifted by such variables as inaccurate measurement of the beam crossing angle and misalignment of the receiving optics. Over-all, however, the experience to date indicates that reproducable LDV measurements are possible for transonic flows that are accurate to well within 1% of the mean flow velocity.

Results and Analysis

The results of the analytical and experimental investigation are summarized and compared in Figs. 6–11. The results are

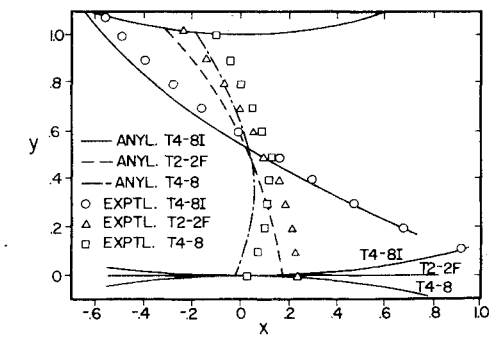

Fig. 9 Comparison of static pressure sonic lines and analytical sonic lines in nozzles T4-8I, T2-2F, and T4-8.

§ One analytical estimate predicts a lag of about 4–5% for 2 μ particles near the throat of the T6-6 nozzle.

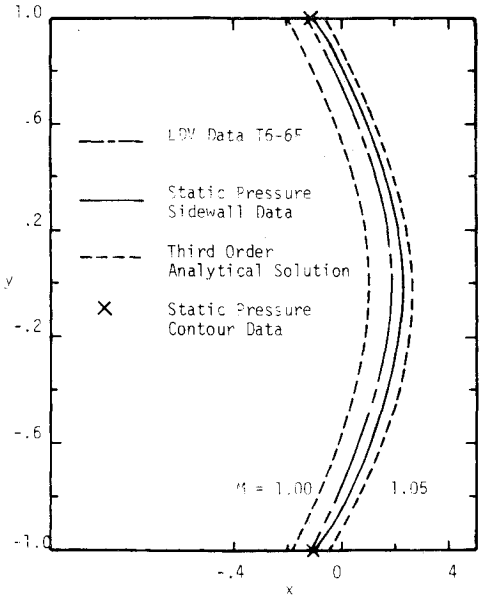

Fig. 10 Comparison of static pressure, LDV, and analytical sonic line location in nozzle T6-6.

presented in terms of sonic line locations for the nozzle configurations listed in Table 1. The experimental sonic lines are located by linear interpolations between measured values. Results are compared from five sources, namely 1) third-order analytical solution with $\eta = 1$, 2) wall-static pressure measurements along the nozzle contour, 3) wall-static pressure measurements on one nozzle sidewall, 4) LDV measurements using peak values of histograms for nozzles T6-6F and T4-8, and 5) the experimental data of Jacobs[18] for nozzle T2-2F. More complete static pressure data with comparisons throughout the transonic range are contained in Ref. 7.

In Fig. 6 the static pressure sonic line location is compared with the data of Jacobs and with the analytical sonic line and the Mach 1.05 line for nozzle T2-2F. The experimental sonic line is downstream approximately 0.06 units from the theoretical sonic line, while the shapes of the two sonic lines are nearly identical. This slight shape difference near the nozzle contours is attributed to the effect of boundary layer on the measured static pressures and the fact that the analytical series solution becomes less accurate as y increases. Figure 6 is representative of the comparison between the experimental static pressure data and the analytical solution for each of the 13 nozzles. Throughout the transonic region the experimental Mach number at a point is typically 1–4% below the theoretical Mach number at that point, so that the experimental sonic line is typically between the $M = 1.0$ and $M = 1.05$ isomachs from the analytical solution.

Figure 7 compares the static pressure sonic line locations for nozzles with nondimensional radii of curvature of 6, 3, and 1.5. The indicated nozzle contours are to scale with respect to the sonic lines. The differences in sonic line location are small and are primarily near the contoured wall, as would be expected.

Comparisons of static pressure sonic line locations between nozzles T6-6 and T6-6F, and between nozzles T3-3 and T3-3F show only very slight differences near the contour boundaries. Those results indicate that the plane of a symmetry in a symmetrical nozzle can be replaced by a flat surface with only a small effect on the flow near the contour boundaries. Those comparisons are contained in Ref. 7.

In contrast, Figs. 8 and 9 compare the static pressure sonic line location for a series of unsymmetric nozzles, and demonstrate large shifts in the sonic line location which results from small changes in one boundary. Figure 9 also includes the analytic sonic line locations which compare well with the experimental locations and show the general shift of 1–4% as noted earlier.

In interpreting the geometries in Fig. 8, note that if nozzle T6-6F is considered as an unsymmetrical nozzle rather than half of a symmetrical nozzle, it is designated T12-∞. Similarly, in Fig. 9 the nozzle T2-2F should be considered as unsymmetric nozzle T4-∞. Thus, the comparisons are for a fixed upper nozzle contour and a lower contour that varies from a large concave radius of curvature to a flat plate to a large convex radius of curvature. The figures are to scale.

As can be seen from the figures, the results are dramatic. In all cases, small variations in the lower boundaries change the sonic lines significantly near both contours. In Fig. 8 the sonic point on the lower contour has been moved axially approximately 20 times the vertical distance by which the lower boundary was changed.

The agreement between the analytical and experimental sonic lines is excellent considering the assumptions that have been made, and the measurement uncertainty. As indicated in Ref. 19 there is a tendency for static pressure measurements to be high due to finite static pressure hole sizes. A limited experimental study by the authors confirms that general result and although not completely conclusive, indicates that the error due to the 0.018 in. diam taps used in the study is less than 0.4% in Mach number. A correction would shift the measured sonic line to the left. Additional measurement uncertainty could result in a maximum of $\pm 1.25\%$ shift in Mach number, but is probably much less.

The uncertainty in the theoretical sonic line location results from the fact that the boundary layer on the nozzle sidewalls, boundary layer on the nozzle contour, viscous dissipation, and heat transfer have been neglected in the analysis. This is one of those rare cases in which each of the effects, if considered, would shift the theoretical sonic line in the same direction; that is, to the right. Thus, although the effects are individually small, they are additive, and collectively account for most of the difference between the theoretical and measured values. Other effects such as thermal contraction of nozzle components during a run and condensation of water vapor (and possibly CO_2) were considered and found to have an unmeasurably small effect on the location of the theoretical sonic line.

Further error results from the fact that truncated series are used to compute the theoretical result. As already noted, the error here is larger near the nozzle boundaries and is a function of the nozzle geometry.

The difference in the experimentally measured sonic line and the experimental sonic line reported by Jacobs (Fig. 6) is probably because Jacobs' nozzle was physically larger than the one used in this investigation. Jacobs' data is closer to the theoretical solution (which ignores boundary layer) than the static pressure data of this study. This is as would be expected since the effects of the boundary layer particularly the sidewall boundary layer, do not scale.

Figures 10 and 11 are a comparison of sonic line locations from LDV data, static pressure data, and the analytical solution for nozzles T6-6 and T4-8, respectively. For the LDV data the peak Mach numbers (most abundant in the array of 1000 data samples taken at each point) have been used to construct the sonic line. As can be seen, the LDV data fall between the static pressure data and the analytical solution with a 1–2% difference between the LDV data and the static pressure data.

Summary

Two-dimensional transonic nozzle flows have been examined both analytically and experimentally. The analytical model is based on a Taylor series expansion around a Mach number of one in terms of the wall geometries at the minimum area cross section of the flow. The method was specifically developed to treat both two-dimensional and annular flow passages with unsymmetric wall geometries. The method is comparatively straight forward and fast on a computer and provides accurate

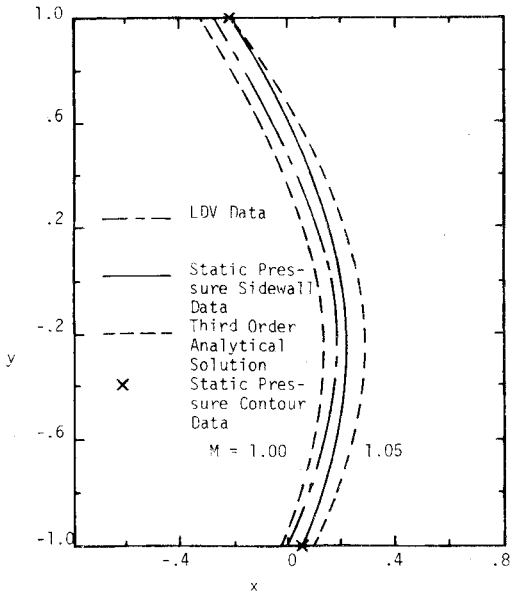

Fig. 11 Comparison of static pressure, LDV, and analytical sonic line location in nozzle T4-8.

solutions for a wide range of geometries of practical significance.

In the experimental investigation, sidewall and contour static pressure data were recorded for thirteen two-dimensional nozzle configurations. LDV data have also been recorded for two of those configurations. The configurations were chosen as a result of the analytical study and included both symmetric and unsymmetric configurations. All nozzle contours were constructed from stainless steel machined into circular arcs. Plexiglas plates were used as sidewalls and were placed 1 in. apart. Pressure measurements were made with 0.018 in. diam pressure taps.

For all nozzles examined, the experimental sonic line was shifted downstream from the inviscid analytical sonic line by 1–4%. This shifting has been attributed primarily to boundary layer on the sidewalls and contours. The LDV data fell between the static pressure data and the analytical data. The results confirm that accurate LDV measurements to within 1% of the actual mean flow velocity are possible and practical in steady transonic flows.

Investigation of several unsymmetric contours illustrates the nonlinearity and sensitivity of some transonic flows. Small changes in one boundary may produce a large shift in the sonic line location. Also, the sonic line location for some geometries is dramatically different from the one-dimensional uniform flow that is often assumed.

References

[1] Sauer, R., "General Characteristics of the Flow through Nozzles at Near Critical Speeds," TM 1147, 1947, NACA.

[2] Hall, I. M., "Transonic Flow in Two-Dimensional and Axially-Symmetric Nozzles," *Quarterly Journal of Mechanical and Applied Mathematics*, Vol. XV, Pt. 4, Nov. 1962, pp. 487–508.

[3] Kleigel, J. R. and Levine, J. N., "Transonic Flow in Small Throat Radius of Curvature Nozzle," *AIAA Journal*, Vol. 7, No. 7, July 1969, pp. 1375–1378.

[4] Levine, J. N. and Coats, D. E., "Transonic Flow in a Converging-Diverging Nozzle," CR 111104, Sept. 1970, NASA.

[5] Moore, A. W. and Hall, I. M., "Transonic Flow in the Throat Region of an Annular Nozzle with an Arbitrary Smooth Profile," ARC Rept. and Memo. 3840, Jan. 1965.

[6] Thompson, H. D. and Flack, R. D., "Transonic Flow Computation in Annular and Two-Dimensional Nozzles," RD-73-21, Dec. 1973, U.S. Army Missile Command, Huntsville, Ala.

[7] Flack, R. D. and Thompson, H. D., "An Experimental and Analytical Investigation of Internal Transonic Flow," RD-73-20, Oct. 1973, U.S. Army Missile Command, Huntsville, Ala.

[8] Serra, R. A., "The Determination of Internal Gas Flows by a Transient Numerical Technique," Ph.D. thesis, June 1970, Department of Mechanical Engineering, Rensselaer Polytechnic Inst. Troy, N.Y.

[9] Wehofer, S. and Moger, W. C., "Transonic Flow in Conical Convergent and Convergent-Divergent Nozzles with Nonuniform Inlet Conditions," AIAA Paper 70-635, San Diego, Calif., 1970.

[10] Brunell, R. D., "Numerical Solutions for Compressible Flow in Planar Converging-Diverging Ducts," Ph.D. thesis, June 1970, Department of Aerospace and Mechanical Engineering, Notre Dame University, Notre Dame, Ind.

[11] Prozan, R. J. and Kooker, D. E., "The Error Minimization Technique with Application to a Transonic Nozzle Solution," *Journal of Fluid Mechanics*, Vol. 43, No. 2, Aug. 1970, pp. 269–277.

[12] Holt, M., "The Design of Plane and Axisymmetric Nozzles by the Method of Integral Relations," *Transactions of Symposium Transsonicum*, ed. by K. Oswatitsch, Springer-Verlag, Berlin, 1964.

[13] Liddle, S. G. and Archer, R. D., "Transonic Flow in Nozzles Using the Method of Integral Relations," *Journal of Spacecraft and Rockets*, Vol. 8, No. 7, July 1971, pp. 722–728.

[14] Hopkins, D. F. and Hill, D. E., "Effect of Small Radius of Curvature on Transonic Flow in Axisymmetric Nozzles," *AIAA Journal*, Vol. 4, No. 8, Aug. 1966, pp. 1337–1343.

[15] Hopkins, D. F. and Hill, D. E., "Transonic Flow in Unconventional Nozzles," *AIAA Journal*, Vol. 6, No. 5, May 1968, pp. 838–842.

[16] Friedrichs, K. O., "Theoretical Studies on the Flow through Nozzles and Related Problems," 82.1R, AMG-NYU 43, 1944, New York University, New York.

[17] Morden, D. B. and Farquhar, B. W., "Transonic Flow in Unconventional Nozzles," *AIAA Journal*, Vol. 7, No. 8, Aug. 1969, pp. 1661–1662.

[18] Jacobs, W., "Geswindigheitsverteilungen in Zweidimensionalen gekrümmten Lavaldüsen," *Jahrbuch wiss. Gesellschaft Luftfahrt*, 1954, pp. 57–62.

[19] Back, L. H., Massier, P. F., and Gier, H. L., "Comparison of Measured and Predicted Flows through Conical Supersonic Nozzles with Emphasis on the Transonic Region," *AIAA Journal*, Vol. 3, No. 9, Sept. 1965, pp. 1606–1614.

[20] Cuffel, R. F., Back, L. H., and Massier, P. F., "Transonic Flowfield in a Supersonic Nozzle with Small Radius of Curvature," *AIAA Journal*, Vol. 7, No. 7, July 1969, pp. 1364–1366.

[21] Back, L. H. and Cuffel, R. F., "Flow Coefficients for Supersonic Nozzles with Comparatively Small Radius of Curvature Throats," *Journal of Spacecraft and Rockets*, Vol. 8, No. 2, Feb. 1971, pp. 196–198.

[22] Back, L. H., Cuffel, R. F., and Massier, P. F., "Influence of Contraction Section Shape and Inlet Flow Direction on Supersonic Nozzle Flow and Performance," *Journal of Spacecraft and Rockets*, Vol. 9, No. 6, June 1972, pp. 420–427.

[23] Zammit, R. E., Pedigo, M. K., and Stevenson, W. H., "A High Frequency Burst Signal Processor for Laser Velocimeter Applications" RD-CR-74-4, Jan. 1974, U.S. Army Missile Command, Huntsville, Ala.

[24] Yanta, W. J., "Measurements of Aerosol Size Distributions with a Laser Doppler Velocimeter (LDV)," AIAA Paper 73-705, Palm Springs, Calif., 1973.